Publications of the Astronomical Society of the Pacific, **126**:398–408, 2014 April

The K2 Mission: Characterization and Early Results

Steve B. Howell,[1] Charlie Sobeck,[1] Michael Haas,[1] Martin Still,[1,2] Thomas Barclay,[1,2] Fergal Mullally,[1,3] John Troeltzsch,[4] Suzanne Aigrain,[5] Stephen T. Bryson,[1] Doug Caldwell,[1,3] William J. Chaplin,[6,7] William D. Cochran,[8] Daniel Huber,[1,3] Geoffrey W. Marcy,[9] Andrea Miglio,[6,7] Joan R. Najita,[10] Marcie Smith,[1,3] J. D. Twicken,[1,3] and Jonathan J. Fortney[11]

Received 2014 February 08; accepted 2014 March 07; published 2014 April 11

ABSTRACT. The K2 mission will make use of the *Kepler* spacecraft and its assets to expand upon *Kepler's* groundbreaking discoveries in the fields of exoplanets and astrophysics through new and exciting observations. K2 will use an innovative way of operating the spacecraft to observe target fields along the ecliptic for the next 2–3 years. Early science commissioning observations have shown an estimated photometric precision near 400 ppm in a single 30 minute observation, and a 6-hr photometric precision of 80 ppm (both at V = 12). The K2 mission offers long-term, simultaneous optical observation of thousands of objects at a precision far better than is achievable from ground-based telescopes. Ecliptic fields will be observed for approximately 75 days enabling a unique exoplanet survey which fills the gaps in duration and sensitivity between the *Kepler* and TESS missions, and offers prelaunch exoplanet target identification for JWST transit spectroscopy. Astrophysics observations with K2 will include studies of young open clusters, bright stars, galaxies, supernovae, and asteroseismology.

1. INTRODUCTION

The NASA *Kepler* mission was launched in 2009 and collected wide-field photometric observations of a single field of view located in the constellations of Cygnus and Lyra (Borucki, et al., 2010). The data obtained by *Kepler* has revolutionized the study of exoplanets and astrophysics by providing high-precision, high-cadence, continuous light curves of tens of thousands of stars. The loss of two reaction wheels on the *Kepler* spacecraft has ended the primary mission data collection and the project is currently analyzing the final year of observations. The *Kepler* project has thus proposed the K2 mission to NASA via the 2014 Senior Review process. K2 is the name chosen for this new mission concept to allow a distinction between it and the nominal *Kepler* mission. K2 can be thought of as being a 2-wheel *Kepler*, the second *Kepler* mission, or as an analogy to the enigmatic and challenging mountain of the same name. A decision on funding K2 will be reached in late 2014 spring and, if positive, K2 will begin official operations near 2014 June 1, making observations for approximately the next 2 years along the lines discussed in this paper.

The *Kepler* spacecraft, with its 0.95-m Schmidt telescope and 110 square degree field of view imager (4″ pixels), is in a heliocentric orbit currently about 0.5 AU from the Earth. Like *Kepler*, the K2 mission is founded on the proven value of long-baseline, high-cadence, high-precision photometry and exploits a large field of view to simultaneously monitor many targets.

The K2 mission plan is to point near the ecliptic, sequentially observing fields as it orbits the Sun. This observing strategy regularly brings new, well-characterized target regions into view, enabling observations of scientifically important objects across a wide range of galactic latitudes in both the northern and southern skies. K2 will perform a series of long, ecliptic-pointed campaigns that use the proven *Kepler* infrastructure to conduct new research into planet formation processes, young stars, stellar activity, stellar structure and evolution, and extragalactic science. Herein, we present the details of our new method of spacecraft operation and some early results that characterize the scientific abilities of K2.

2. THE K2 MISSION

The K2 mission is driven by the spacecraft's ability to maintain pointing in all three axes with only two reaction wheels (Putnam & Wiemer, 2014). Figure 1 shows a schematic of

[1] NASA Ames Research Center, Moffett Field, CA 94035.
[2] Bay Area Environmental Research Inst., 560 Third St., West Sonoma, CA 95476.
[3] SETI Institute, 189 Bernardo Avenue, Suite 100, Mountain View, CA 94043.
[4] Ball Aerospace and Technology Corp., P.O. Box 1062, Boulder, CO 80306.
[5] Sub-department of Astrophysics, Department of Physics, University of Oxford, Oxford OX1 3RH, UK.
[6] School of Physics and Astronomy, University of Birmingham, Edgbaston, Birmingham, B15 2TT, UK.
[7] Stellar Astrophysics Centre (SAC), Department of Physics and Astronomy, Aarhus University, Ny Munkegade 120, DK-8000 Aarhus C, Denmark.
[8] McDonald Observatory & Department of Astronomy, The University of Texas at Austin, Austin, TX 78712.
[9] University of California, Berkeley, CA 94720.
[10] National Optical Astronomy Observatory, 950 N. Cherry Avenue, Tucson, AZ 85719.
[11] Department of Astronomy and Astrophysics, University of California, Santa Cruz, CA 95064.

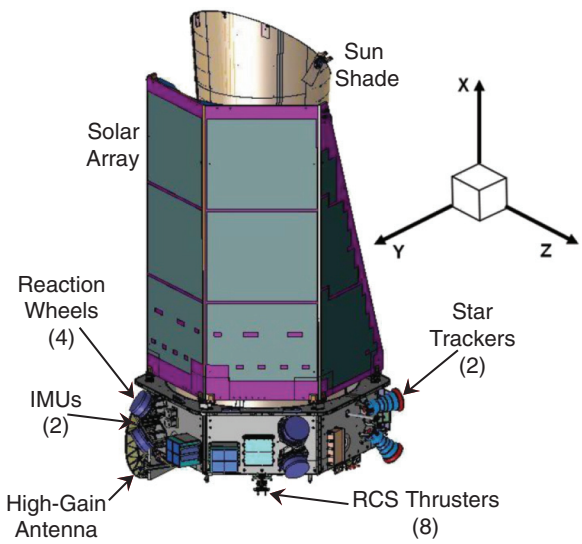

FIG. 1.—*Kepler* spacecraft coordinate system.

the spacecraft and the X-, Y-, and Z-axes. Solar pressure represents the only disturbing force, which is controlled by wheels about the Y- and Z-axes and by thrusters about the X-axis. Sustained, stable pointing requires that the X-axis disturbing force (roll axis) be minimized for extended periods. This is accomplished by pointing in the orbital plane, where the apparent motion of the Sun (caused by the spacecraft's orbital motion while inertially pointed) follows the spacecraft line of symmetry in the X-Y plane over the course of a campaign, providing a balanced pressure and minimizing the X-axis disturbance.

By carefully selecting the initial roll angle and correcting for drift every 12 hr, the spacecraft can remain stable in roll during the observation period. Meanwhile, the reaction wheels control pointing about the Y- and Z-axes as in the *Kepler* mission, absorbing the torque generated by the solar radiation pressure. The accumulated momentum is dumped through thruster firings every two days. This operating mode provides a fuel budget that allows for a 2–3 year mission duration. Starting in 2013 October, the operations team has demonstrated and refined the techniques needed to fly the spacecraft using this approach, performed an on-orbit demonstration of performance, and delivered early commissioning science (§ 5).

K2 has begun to observe a series of independent target fields (campaigns) in the orbital plane (essentially the ecliptic plane). The duration of each observing campaign is limited by solar illumination constraints on the spacecraft, bounded by power constraints on one end and aperture illumination on the other. Science observations are limited to about 75 days per field, as illustrated in Figure 2.

A generic K2 observing campaign timeline is shown in Figure 3. Each K2 campaign will start when the target field comes into view. A checkout period will be used to upload target tables and configure the spacecraft attitude control system for the

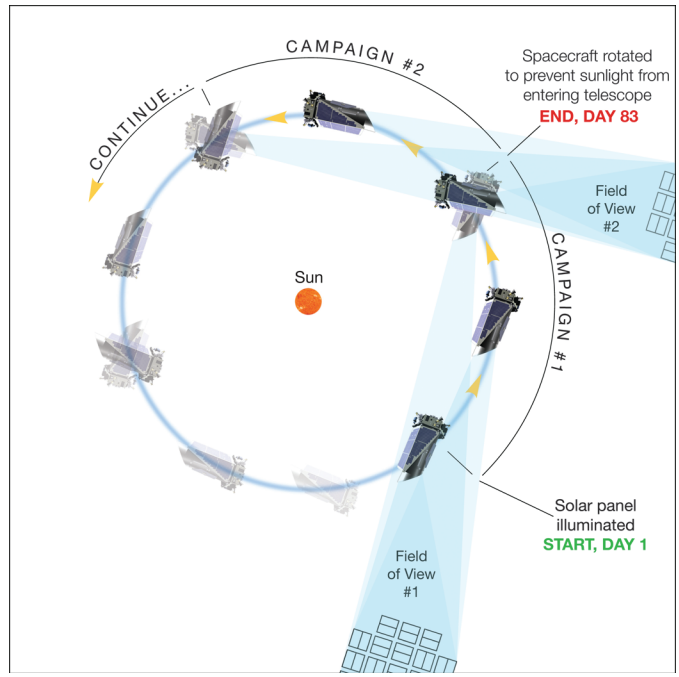

FIG. 2.—The K2 mission will observe sequential ecliptic campaigns with a duration of ~83 days, where 75 days are dedicated to science.

upcoming campaign. The spacecraft will then be turned to the new science attitude to collect pointing alignment data, which are downlinked to the ground stations and to the project in near real-time. Analysis of these data will then allow adjustments to the spacecraft configuration as needed and start the science observations for the campaign. To maximize the unbroken observation period and reduce operational cost/complexity, all science data will be stored onboard until the end of the campaign. The spacecraft will then autonomously turn to point the high-gain antenna back toward the Earth and the science data downlinked. Afterwards, the next campaign checkout period will begin. During science observations, in-situ health and safety checks will be performed periodically and fault protection will monitor

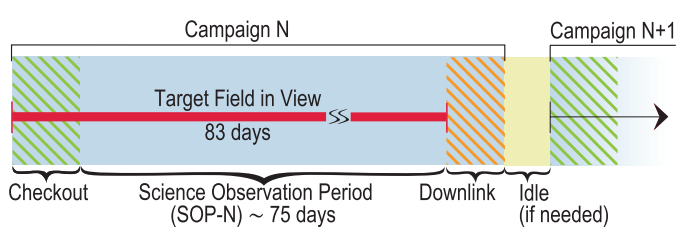

FIG. 3.—Schematic representation of a typical K2 campaign showing how each will provide a long, uninterrupted science observation period. An initial checkout period assures precise initial pointing, while all data are returned at the end of the campaign during an approximately 2-day downlink period. Idle time can be inserted between campaigns to allow flexibility in choosing the next field-of-view.

spacecraft performance, placing the spacecraft into safe-mode in the event of a significant anomaly.

K2 retains the *Kepler* point-and-stare observing approach, minimizes operational changes, and utilizes the data processing infrastructure with modifications limited to those required to accommodate the larger pointing drift and pointing control artifacts. The quantity of the data delivered from each campaign will be far less than any *Kepler* quarter, as K2 will be observing only $\sim 10,000$ targets, not the 150,000 observed in the nominal mission. Spacecraft communications will only slightly degrade over the anticipated K2 lifetime (2–3 years) and will have no effect on the science data quality discussed here. All spacecraft operations are managed through parameter table updates, and no flight software changes are required. Aside from the failed reaction wheels and the loss of two CCD modules (No. 3 in 2010 January and No. 7 in 2013 January), the spacecraft has shown little performance degradation and the remaining reaction wheels show no signs of wear. Each K2 imaging science campaign will cover ~ 105 square degrees and be self-contained.

3. K2 KEY SCIENCE GOALS

The K2 mission was conceived to repurpose the *Kepler* spacecraft within the limitations imposed by two-wheel operations, and was influenced by the large community response to a 2013 summer call for white papers.[12] K2 is a multi-field, ecliptic-pointed mission that will allow observations of thousands of targets covering the science areas of transiting exoplanets, clusters of young and pre-main sequence stars, asteroseismology, AGN variability, and supernovae.

In each year of operation, K2 will observe approximately 40,000 targets ($\sim 10,000$ per field of view) spread over four fields of view. K2 will collect data at 30-minute and 1-minute cadences and will produce 80-ppm photometry for 12th magnitude stars on 6-hr time scales (§ 5). K2 will observe in both the northern and southern sky, in and out of the plane of the Galaxy and, over two years, cover ten times more sky area than the original *Kepler* mission.

The K2 mission will provide many opportunities for new discoveries through its observation of targets and Galactic regions not accessible to *Kepler* (e. g., Beichman et al. 2013). K2 is a community-driven observatory with targets chosen from peer-reviewed proposals; even the K2 fields will be chosen in coordination with the community (§ 4). As such, we can not know ahead of time the exact number or type of targets K2 will observe. No predetermined set or type of targets is part of the mission concept. The peer-review process will determine the actual target mix for each K2 field of view and thus what science will be possible from the observations made in each campaign. Ecliptic fields which lie out of the Galactic plane are likely to be dominated by extragalactic targets while those in dense star forming regions will probably receive proposals aimed mainly at young stars and clusters. Additional science results are also expected through observations of unique sources such as solar system objects, black-hole and x-ray binaries, young massive stars, and numerous variable and pulsating stars. K2 will use its unique assets to make observations capable of answering important questions in a number of science areas that are briefly highlighted below.

3.1. K2 Observations of Transiting Exoplanets

Kepler discovered that planets are common with small ones being plentiful (Howard et al., 2012). To move from discovery to characterization, host stars and their planets are needed which enable followup yielding detailed properties. The K2 photometric precision will be lower and the time per field shorter than the *Kepler* mission; however, K2 has the potential to become a powerful exoplanet finder, easily exceeding the capabilities of ground-based surveys by large margins in sensitivity, field-of-view, and continuous time coverage. Figure 4, based on early science results (§ 5), illustrates the ability of K2 to detect planets as functions of stellar type and exoplanet radius.

3.1.1. Observations of Exoplanets Orbiting Low-Mass Stars

M dwarfs offer a unique opportunity to progress from planetary discovery to characterization. The proximity of these host stars and the large photometric transit depths allow a wide variety of additional observations aimed at characterizing the atmospheres and properties of such planets. For example, the

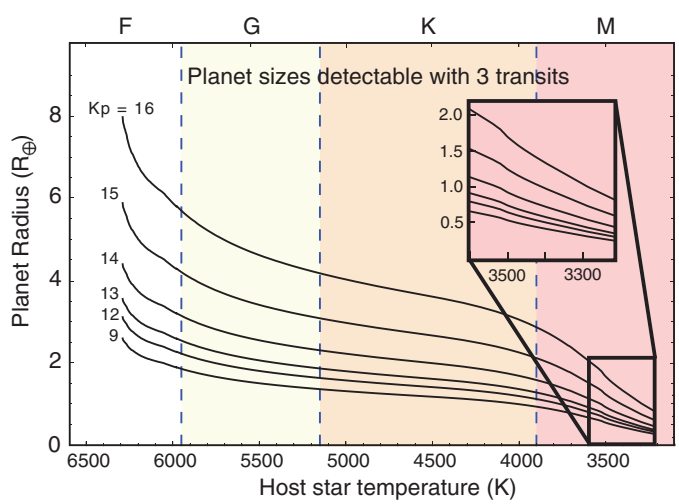

FIG. 4.—K2 will detect small, short-period planets around cool dwarfs. Using three transits as a metric for detecting short-period candidate exoplanets (based on K2 photometric performance as described in § 5) the planet-detection thresholds for various dwarf-star types are shown for a range of *Kepler* magnitudes (Kp~ R-band). For high signal-to-noise ratio events, two transits are sufficient to support the detection of small Habitable Zone planets orbiting M dwarfs.

[12] The community-produced white papers are available at http://Keplerscience.arc.nasa.gov/TwoWheelWhitePapers.shtml.

exoplanet GJ1214b (Charbonneau et al., 2009), while not in the Habitable Zone or rocky, was discovered orbiting a star relatively close to the Sun and lead to many interesting and useful follow-up studies.

The highlighted box in Figure 4 shows the K2 discovery space for small rocky planets ($<1.6\ R_{\rm E}$) orbiting M dwarfs. Note that the rapid decrease in stellar radius beyond spectral type M1V ($T_{\rm eff} < 3600$ K) allows K2 to detect small planets even for the generally faint population of M stars.

The results from the *Kepler* mission point toward a high occurrence rate for small planets closely orbiting M dwarfs (e.g., Dressing & Charbonneau 2013; Gaidos 2013; Kopparapu 2013). Due to their low absolute luminosity, M dwarfs are a local population and their distribution remains approximately uniform across all K2 fields-of-view (Ridgway et al. 2014). K2 can observe approximately 4000 M dwarfs brighter than 16th magnitude per field. From the *Kepler* estimated M dwarf small-planet frequency, it is expected that K2 will discover approximately 100 Earths and Super-earths ($0.8 \leq R_{\rm Planet} \leq 2.0$) per year (~4.5 fields), with a few in the Habitable Zone (defined here as the empirical Habitable Zone; Dressing & Charbonneau [2013]). The larger transit depths of M dwarf planets open the door to a variety of ground- and space-based follow-up observations. The detection of such transits would permit detailed follow-up studies as were done for GJ1214b, providing prelaunch targets for JWST and the next generation of large-aperture ground-based telescopes.

3.1.2. Observations of Exoplanets Orbiting Bright Stars

The main objective of the *Kepler* mission was to measure the occurrence rate of planets around Sun-like stars, particularly for Earth-size planets. *Kepler* target stars were generally faint (V = 13 to 15) in order to build a large enough sample that could be searched continuously for four years. The *Kepler* results, that exoplanets are common, is crucial for the design of future instrumentation and missions that will make the next leap in exoplanetary science—exoplanet characterization. To accomplish this, the nearest and brightest stars, harboring the most readily studied planets and planetary systems, need to be discovered.

Bright stars (V < 12) offer far more information than simply telling us about the mere existence of a planet. A significant open question in exoplanetary science concerns the interior structure and composition of planets smaller than $2\ R_{\rm E}$, irrespective of orbital location. Most planets below $1.4\ R_{\rm E}$ seem to be rocky (Marcy et al. 2014), while planets larger than $2\ R_{\rm E}$ appear to be volatile rich mini-Neptunes. However, the densities are known for only a handful of planets between these bounds.

Transits detected on bright stars by K2 will enable precise Doppler spectroscopy, to provide planetary masses and densities, and spectroscopic characterization of planetary atmospheric properties. Bright stars are also amenable to high-resolution spectroscopy, high-resolution imaging, asteroseismology, interferometry, proper motion, and parallax measurements, all useful to determine the host star properties

The number of bright dwarfs (V < 12) that K2 can observe in each campaign fluctuates throughout the year from around 3000 to over 7000. Figure 5 shows the detectable planet sizes that can be found in short-period orbits during a typical campaign. It should be noted that about 40% of the planet candidates found by *Kepler* have periods less than eight days and about half of these have sizes less than $2\ R_{\rm E}$ (Ciardi et al. 2013). Assuming 50% of the targets are V < 12 stars, K2 will observe approximately 20,000 bright stars in a given year and it should find about 50 potentially rocky planet candidates based on *Kepler* statistics. The ecliptic is already home to a number of bright exoplanet host stars: 15 are bright (V = 5–8) with short-period RV planets and 23 are transiting systems.

3.2. K2 Observations of Open Clusters

MOST, CoRoT, and *Kepler* have all made contributions to open-cluster science, but for limited samples and for distant, faint, and crowded clusters. K2 campaigns (§ 4) are planned to survey a rich area of the sky, containing the brightest and best characterized clusters (see Table 1). Much is already known about these clusters and associations, including cluster membership and stellar properties.

In these clusters, K2 can survey a few thousand bright pre- and early main sequence stars down to $0.15\ M_{\odot}$). Assuming a photometric precision of 80 ppm on transit timescales for a 12th

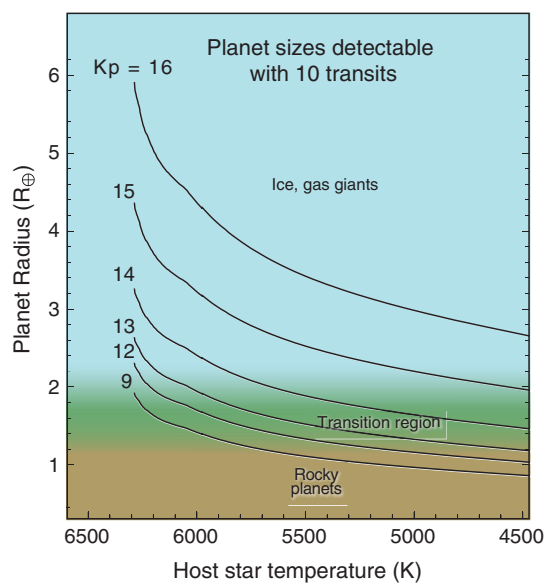

FIG. 5.—K2 will discover exoplanets which probe the transition and rocky regimes for G dwarfs (to 13th magnitude) and for cooler stars. Based on *Kepler* statistics and the expected photometric performance (§ 5), K2 is expected to detect ~50 planet candidates per year with orbital periods <8 days and radii $<2\ R_{\rm E}$.

TABLE 1
K2 Open Clusters

Cluster	Age (Myr)	Distance (pc)	K2 Campaign (Proposed)	Ref.
Taurus	2	140	4	Rebull et al. (2012)
Upper Sco	10	130	2	Pecaut et al. (2012)
M21	12	1200	9	Piskunon et al. (2011)
M18	32	1300	9	Santos-Silva & Gregorio-Hetem (2012)
M25	92	620	9	Piskunon et al. (2011)
M35	100	800	0	McNamara et al. 2012
M45	125	135	4	Bell et al. (2012)
NGC 1647	150	547	10	Piskunon et al. (2011)
NGC 6716	150	547	7	Piskunon et al. (2011)
Hyades	630	46	4	Schilbach & Roser (2012)
M44	630	160	5	Boudreault et al. (2012)
M67	4300	908	5	Dias et al. (2012)

magnitude star, K2 can comfortably detect planets down to 2.5 $R_{\rm E}$, the size of Super-Earths, in all the clusters listed in Table 1. The incidence of short-period planets around field stars (Fressin et al. 2013; Petigura et al. 2013) suggests that a few transiting hot Jupiters and Neptunes will be found per campaign, as well as several tens of Super-Earths and smaller planets assuming ∼1500 cluster members are observed (see § 3.1). To date, only a handful of planets have been detected in open clusters (Quinn et al. 2012; Meibom et al. 2013; Brucalassi et al. 2014). These discoveries indicate that the incidence of large planets in clusters is similar to that around field stars. The K2 mission has the ability to determine if small planets are as common in open clusters as in the field. Planetary systems discovered in the Hyades will be particularly valuable for follow-up studies with JWST, being bright and only 46 pc from the Sun.

The past decade has seen an increase in the number of rotation-period measurements available for pre-main sequence and early main sequence stars, but theoretical models still struggle to reproduce all the available data (e.g., Gallet and Bouvier 2013). Typical rotation periods for young cluster stars range from 1 to 20 days (Irwin & Bouvier 2009), and have large and distinct modulation amplitudes, easily detectable and distinguished from transit events. K2 observations of many cluster members can provide an essentially complete rotation census in each targeted cluster.

Detached, double-lined eclipsing binaries provide model independent determination of the masses, radii, effective temperatures, and luminosities of both stars from the light and radial velocity curves of the system. CoRoT observations of the open cluster NGC2264 (Gillen et al. 2014) and *Kepler* observations of NGC 6811 (Janes et al., 2013) can be used to estimate that K2 will discover ∼10 new eclipsing binaries per cluster for which the masses and radii of both components can be determined to about 1%. The continuous sampling achievable by K2 also enhances the sensitivity to moderate period (i.e., 8–20 days) eclipsing binaries, enabling their (spin) evolution to be studied as a function of the mutual interaction between the two stars.

The use of asteroseismology can significantly advance our understanding of stellar evolution, stellar-interior physics, and stellar populations (Chaplin & Miglio 2013). Nowhere will this be more powerful then when used to combine high-precision photometric observations with strong prior information on age, distance, and metallicity in clusters that span a wide range in mass, chemical composition, and evolutionary state. K2 observations of bright stars within clusters, e.g., O-B stars (Aerts et al. 2003, 2013; Degroote et al. 2010) or A and F pulsators (Michaud & Richer 2013) can yield results on radiative levitation and element depletion processes, and the onset of near-surface convection, and allow comparisons of distance scales for various cluster stars using the standard pulsating variables such as RR Lyrae stars or Cepheids.

Studies of Galactic star populations with K2, both in clusters and in the field, could measure radii, masses, distances, and ages of thousands of giants providing a unique asteroseismic survey spanning a wide range of vertical and radial structure in our Galaxy. These data would allow Galactic mass and age gradients to be studied and characterized for a wide range of populations, out to similar distances to those probed by red-giants in the *Kepler* field. Detections in the *Kepler* and CoRoT fields are already being utilized (e.g., Miglio et al. 2013; Stello et al. 2013), but their fixed pointings carry obvious limitations that will be lifted for K2 (Fig. 6). Combined with astrometric data from Gaia, K2 observations of field red giants would provide a valuable community dataset (Chaplin & Miglio 2013).

3.3. Observations of Star-Forming Regions

Understanding how giant planets form and accumulate their gaseous envelopes is still an observational frontier. K2 campaigns will study star-forming regions providing the opportunity to test planet-formation theories by probing planetary properties during formation or immediately thereafter. Standard

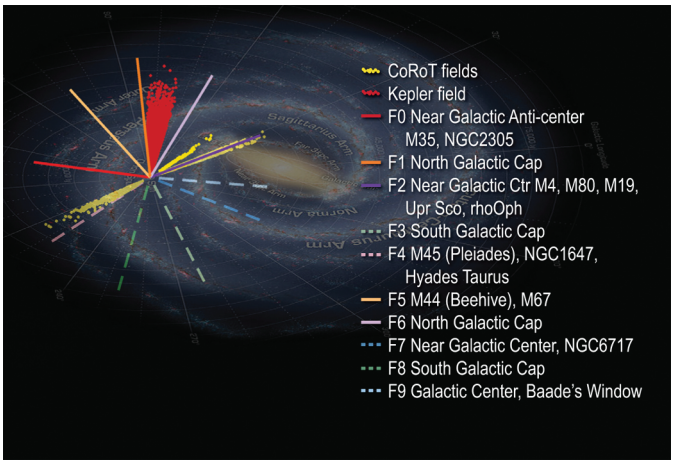

FIG. 6.—The Galactic distribution of oscillating red giants accessible to K2 is compared to those observed by *Kepler* and CoRoT. In this cartoon view of the Galaxy, we see that K2 fields will increase the distribution of environments in which asteroseismology can be applied in order to measure the masses, radii, distances, and ages of stars.

core accretion (e.g., Lissauer et al. 2009) predicts that protogiant planet sizes are large (50–100 R_J) during the slow-gas accretion phase. After accretion has ended, the planet contracts to a more modest size (~1.1 to 1.6 R_J) for a 1 M_J planet. The actual value of the planetary radius at this young age is extremely sensitive to how efficiently the planet radiates away accretion energy. Measuring small planet sizes with K2 will show that the radiation process is extremely efficient and this energy is easily lost: planets start off their life with a "cold start". Detecting much larger planets with K2 might indicate an earlier phase of evolution or that the accretion process is not efficient in radiating energy away.

The migration of hot Jupiters early in a star's life (less than 1 Gyr) is believed to result from one of two mechanisms: migration within the protoplanetary disk ("disk migration"; e.g., Raymond et al. 2006) or some mechanism that dynamically produces highly eccentric orbits, evolved via tides ("dynamical migration"; e.g., Albrecht et al. 2012). These two scenarios deliver the hot Jupiters at different times during the star's evolution: promptly, or delayed to greater than 0.5 Gyr by tidal evolution. Therefore, any K2 measured orbital periods of Jupiter-mass planets will be a sensitive test of hot- versus cold-start models and migration scenarios (see Marley et al. 2007; Spiegel and Burrows 2012). Characterizing planetary systems at the few Myr age of T Tauri stars will explore the dynamical evolution of planetary systems by comparison with the results of more mature planetary systems. Measured abundances of hot Jupiters around young stars can be compared with measurements obtained by *Kepler* for older field stars.

The variability of the young stars is likely to be higher than field stars (Van Eyken et al. 2012), which will provide interesting science in itself, but may impact transit detection and RV follow-up (e.g., Crockett et al. 2012). However, hydrodynamics studies of forming giant planets (e.g., Klahr & Kley 2006; Gressel et al. 2013) suggest that these objects may be more readily detectable than previously believed. For example, in a three-dimensional radiation hydrodynamics study, Klahr (2008) found that the nascent planet is surrounded by a warm pressure-supported bubble with a large pressure scale height ($H/R \sim 0.5$) rather than a thin Keplerian circumplanetary accretion disk ($H/R \leq 0.1$). If such gas/dust bubbles are indeed signposts of giant planet formation, their large scale height would likely make them detectable through a transit signature as they occult the central star. K2 observations of a very large sample of well-characterized young stars during their early formation processes

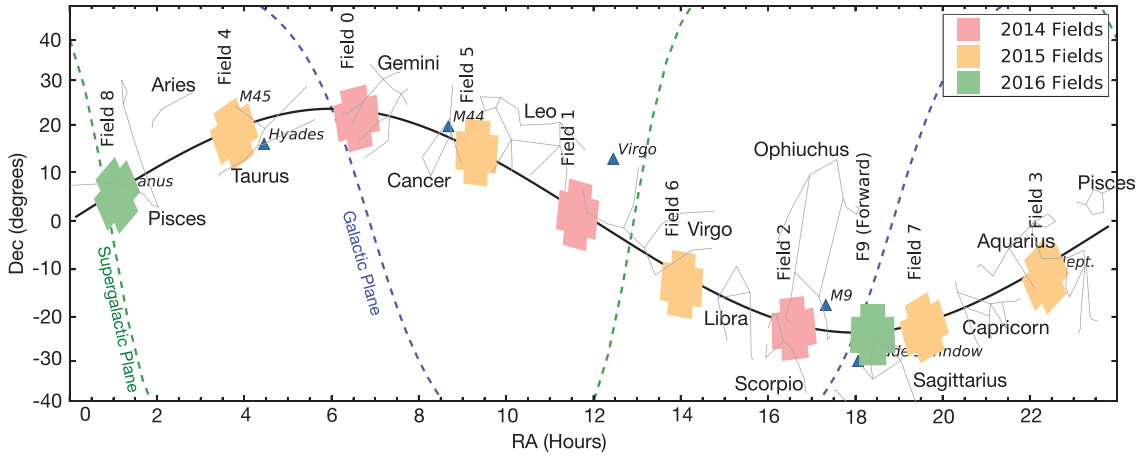

FIG. 7.—The K2 ecliptic observing field sequence was anchored by Field 4, which collects observations of the Pleiades and Hyades clusters in 2015 (see Table 2). Earlier and later fields march around the ecliptic in steps of 83 days as described in Fig. 2. Field 9 is designed to observe along the spacecraft velocity vector (pointing toward the Earth), instead of the standard anti-velocity vector, to provide a unique K2 survey of Baade's window to be used for a microlensing study. This Earth-pointing orientation was chosen to allow simultaneous ground-based support.

would yield valuable information as well as targets for follow-up with ALMA.

3.4. K2 Observations of Variable Extragalactic Sources

Kepler observations of extragalactic sources have allowed the initial exploration of AGN variability on a variety of time scales (hours to months) (Mushotzky et al. 2011). Edelson et al. (2013) and Olling et al. (2013) have found new active galactic nuclei (AGNs) exhibiting low levels of activity, and have discovered at least four supernovae. K2 can provide observations of thousands of galaxies, many well-studied (e.g., COSMOS field), through its observations at high Galactic latitude, areas rich in extragalactic sources.

3.4.1. AGN Variability

Theoretical models (Arevalo et al. 2009; Breedt et al. 2010) suggest that the power spectral densities (PSDs) of accretions disks have spectral indices of -1.4 to -2.0. However, *Kepler* observations provide a few well-determined PSDs yielding slopes of -3.0 (Mushotzky et al. 2011). The steep measured slopes are inconsistent with model predictions, but are based on a small sample. In addition, BL Lac microvariability (0.5–1%) measurements, such as for W2R1926 + 42 observed with *Kepler*, provide evidence for periods of strong flaring and periods of relative quiescence. This type of behavior cannot be fit with the existing simple models for Seyfert galaxies. A larger sample of sources is needed, including various AGN types with varying properties such as luminosity and black-hole mass.

Edelson and Malkan (2012) list 4316 AGNs in the entire sky brighter than J = 16 (R ~ 17) suggesting nearly a dozen bright AGNs will reside in each K2 field. It is likely that K2 will observe over a hundred microvariable extragalactic sources during its mission (Edelson et al. 2013), allowing a broad range of variable AGNs to be observed in statistically significant numbers that will provide robust testing of the current models.

3.4.2. Progenitors of Type Ia Supernovae

Over 20,000 known galaxies brighter than 19th magnitude will be visible per year in K2 fields. K2 observations could allow detection of supernovae for the observed galaxies. Taking the typical observed supernova rate (0.7 supernova/century/ galaxy; Olling et al. 2013), K2 will observe many galaxies for a variety of scientific reasons, some of them, a few tens per year, will contain supernova whose early light curves will be serendipitously collected.

Olling et al. (2013) present a Type Ia supernova light curve obtained with *Kepler*. The continuous light curve coverage starting prior to onset yields unique observations of the early event. This early rise-time information can, for all types of supernovae, tightly constrain the progenitor of the explosion and detail the subsequent shock physics (Woosley et al. 2007; Kasen 2010; Haydon et al. 2010). Theoretical models (Nakar & Sari 2010; Kasen 2010) show that a single degenerate star will cause smooth shock emission in the first few hours to days after the explosion, while double degenerates are expected to brighten monotonically. There are no existing or planned facilities that can provide initial and early rise-time information for supernovae light curves with the precision and time coverage available with K2.

3.5. K2 Microlensing Observations

For the majority of the planets currently detected by microlensing, a parallax determination is needed to determine their masses and distances (Gould 1999; Dong 2009). K2 might provide this missing ingredient by measuring "microlens parallaxes" (Gould & Horne 2013). Planets detected in this manner are particularly interesting because they inhabit a cold region that is inaccessible to other detection methods (Gould & Loeb 1992).

The K2 solar orbit and wide field-of-view make it well suited to measure microlens parallaxes. K2 will see a radically different event from the Earth-based event because it is displaced by approximately 0.5 AU. When combined with ground-based observations, the measured parallax yields the host star and planet masses. K2 could observe as many as 12 microlensed planets in a single campaign (Gould & Horne 2013), enabling the first robust measurement of the mass function of cold, low-mass planets across different stellar populations. One of the most spectacular results from microlensing is the detection of "free-floating" planets. Here too, the microlensing parallax will measure the mass of these objects and confirm their planetary nature.

K2 microlensing results would also provide important input to future microlensing surveys, in particular WFIRST, by estimating the expected yield determining the resources needed for WFIRST follow-up. Field 9 (§ 4, Fig. 7), is a forward looking field, and is ideal for a microlensing study as it is near the Galactic center. Forward looking fields, that is, pointing in the positive velocity vector of the spacecraft, offer the ability of simultaneous Earth-based observations during the K2 observations. However, the Earth and moon enter into the K2 field of view during the 75-day campaign. Our initial planning for Field 9 is likely to consist of shorter visits to dense star fields and to use full-frame readouts of the entire array instead of individual target pixels. This unique K2 campaign will be dedicated to a microlensing investigation and will operate differently than the other campaigns. In order to obtain the highest scientific return from this microlens study, the exact method of field 9 observations will be planned in coordination with the microlensing community.

4. K2 COMMUNITY INVOLVEMENT: FIELD AND TARGET SELECTION AND SCIENCE ARCHIVES

Based upon the the spacecraft abilities, the two-wheel white paper call, and additional community feedback, a series of

ecliptic K2 fields of view have been proposed (Fig. 7). These fields are rich in the types of targets requested by the community. Table 2 lists the planned K2 campaigns, the R.A. and decl. of the center of the field of view, and the date of mid-campaign. The locations of Fields 1 and 2 are now fixed with Fields 3–9 still accepting community input. Each K2 field position needs to be finalized approximately six months prior to its start. The location of each campaign field attempts to optimize the science yield while balancing the spacecraft abilities as well as providing the requisite number of guide stars for the telescope. Maximizing the science, for example, might move a field start or end date a few days to include more stars from a highly proposed cluster. These types of trades in the field position are balanced with the mission concept of providing long-term observations (75 days) at each field and moving from field to field with as few as possible nonscience collection days in between. Details of the location of each field and the method for user input can be found at the Kepler Science Center13.

K2 will observe 10,000–20,000 targets per campaign collected on a 30-minute cadence and an additional 100 targets per campaign collected on a 1-minute cadence. Target numbers are limited by on-board storage and compression, downlink capability, and campaign length. The precise number of targets observed will vary by campaign and will be an optimized trade based upon targets and spacecraft pointing performance. The scientific community will propose all targets for each campaign. The K2 mission will provide a catalog of potential sources within each campaign field based on photometric and astrometric surveys such as Hipparcos, Tycho-2, UCAC-4, 2MASS, and SDSS. The catalog will contain celestial coordinates, proper motions, parallaxes, broadband magnitudes, and inferred K2 bandpass magnitudes, as well as estimates of stellar properties (e.g., effective temperature, surface gravity, and metallicity). Each catalog will be archived at the MAST prior to calls to the community for target proposals. The K2 targets discussed herein and the potential results from our listed key science areas are subject to successful proposals from the community. There will be no restrictions on what type of science may be proposed and no exclusive use period for any K2 data.

K2 has begun making preliminary science observations starting on 2014 March 8 (Campaign 0), moved slightly to include the open cluster M35. Of the $>100,000$ targets proposed for Campaign 0, approximately one-third (with many duplicates) proposed targets are in M35 with the remaining majority being bright stars, galaxies, and M stars. All K2 campaigns will have peer-reviewed target selection; Campaign 0 and 1 targets have already been solicited and submitted with campaign 1 targets under review at present via a project-selected external review panel. Future campaign targets would be solicited through a NASA announcement of opportunity (AO) similar to other NASA guest observer (GO) programs with the proposals reviewed by a NASA appointed external panel. The details of this review process will be formulated and a guest observer (GO) program is anticipated to begin in 2014 summer if the K2 mission is approved.

The K2 mission will deliver all time-series data to a legacy archive hosted at the Mikulski Archive for Space Telescope (MAST; http://archive.stsci.edu/kepler). The K2 archive will reuse the architecture of the *Kepler* archive, with the advantage that it will look and feel much like the *Kepler* archive. Data products will be produced and archived three months after the end of each campaign, allowing the community to rapidly pursue ground-based follow-up and compete for NASA and other funding resources as early as possible. For Campaigns 0–2, calibrated pixels (bias corrected, flat fielded, smear corrected, and with ADU's converted into electrons) will be delivered on this nominal schedule, while the higher-level products will be delivered at a later date in 2014. In support of community-led exoplanet candidate detection, vetting, validation, verification, and follow-up, the Exoplanet Archive (http://exoplanetarchive.ipac.caltech.edu) will host the list of potential exoplanet transit events and associated diagnostic data, as well as provide tools and additional data resources for their exploitation. K2 community support will be provided by the *Kepler* Science Center at the NASA Ames Research Center.[13]

TABLE 2

K2 Campaign Fields

Field	R.A.	Decl.	Date of Mid-Campaign
0	06 47	+21 23	2014 May 4
1	11 38	−01 11	2014 Jul 22
2	16 34	−22 49	2014 Oct 14
3	22 21	−11 37	2015 Jan 5
4	03 46	+18 08	2015 Mar 29
5	09 19	+14 12	2015 Jun 20
6	14 01	−13 16	2015 Sep 11
7	19 34	−22 38	2015 Dec 3
8	01 04	+05 12	2016 Feb 24
9	18 24	−24 12	2016 May 17

NOTE.— Units of right ascension are hours and minutes, and units of declination are degrees and arcminutes.

5. K2 EARLY SCIENCE RESULTS

Based upon a series of spacecraft tests between 2013 October and 2014 February, spacecraft operations were refined to maximize two-wheel performance from K2 and deliver science verification results. These tests have demonstrated all of the functionality required for the K2 mission. Science validation data were collected to characterize K2 mission performance, and are presented here to provide a demonstration of K2's ability to carry out its key science goals.

The K2 photometric precision primarily depends on motion of the spacecraft boresight during timescales shorter than an

[13] Please see http://Keplerscience.arc.nasa.gov/K2.

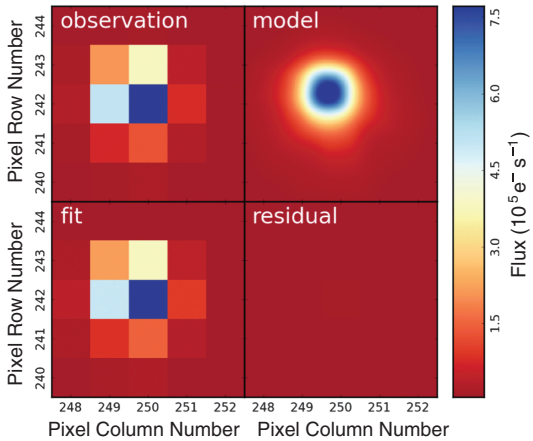

FIG. 8.—The K2 Point-Spread Function (PSF) is well fit by the empirical *Kepler* PSF model. Increased high-frequency movements (jitter) during two-wheel operations increases the *Kepler* PSF FWHM by 2-5% across the detector. From top-left to bottom-right: a 30-minute K2 observation of a 12th magnitude star, the best-fitting *Kepler* PSF model, the best-fit model binned over detector pixels, and the fit residual.

exposure and timescales longer than a single exposure due to motion caused by solar-induced drift. Tests to date have demonstrated spacecraft jitter (high frequency motion) performance comparable to *Kepler* over 30 minutes, or one exposure. The measured full width at half-maximum of the K2 point spread function, a measure of spacecraft jitter, is within 5% of the fine-point *Kepler* point-spread function across the entire field-of-view. Figure 8 provides a fit of the *Kepler* point-spread function to a K2 target close to the spacecraft boresight. Spacecraft jitter during two-wheel operation is therefore generally only a few percent larger than in the three-wheel *Kepler* mission and is not a major concern for K2 photometric precision.

The remaining component of photometric precision is solar-induced drift. This low-frequency motion due to solar pressure and subsequent thruster firings causes targets to drift across detector pixels and is the dominant factor in photometric precision after photon statistics. Thrusters are used to manage momentum by periodically resaturating the reaction wheels and to correct for solar-induced roll-angle drift. Thruster firings kept targets localized to within three pixels during early tests, and later testing demonstrated 1-pixel pointing using focal plane mounted fine guidance sensors.

For the purposes of providing a photometric precision measure that can be compared with the *Kepler* mission, an analysis was conducted on a typical uncrowded 12th magnitude K2 target. The parameters listed here for *Kepler* are not identical to the baseline mission photometric values specific to transit searches as presented in Koch et al. (2010). Here, we make use of the publicly available community software tools. To make our comparison, an identical analysis was performed on a *Kepler* target of the same magnitude. Both light curves are shown in Figure 9. The standard deviations of these two light curves, after normalization by a low-frequency filter, are listed in Table 3.

To compare K2's transit detection sensitivity with *Kepler*'s, motion systematics and stellar variability are removed from these time series using a standard 48-hr Savitzky-Golay filter (Savitzky & Golay 1964). The results are shown in Table 3 for photometric precision over a 6-hr exoplanet transit duration (ζ). *Kepler* operational experience indicates that 7ζ was a reasonable threshold for transit detection and is used for all K2 planet yields estimated above.

Figure 10 provides a comparison of K2's and *Kepler*'s photometric precision as a function of target magnitude. The metric quantifies sensitivity to 6-hr transits and was calculated consistently for both target series. The comparison indicates that current K2 performance is within a factor 3–4 of *Kepler*'s

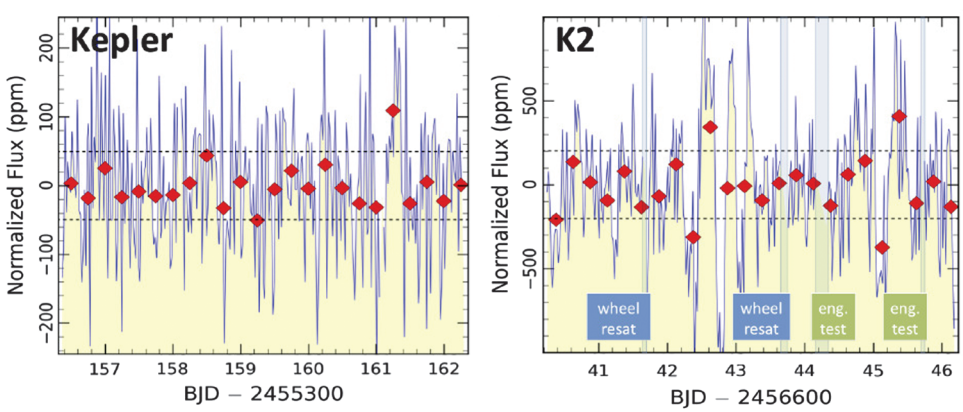

FIG. 9.—The 2013 December on-orbit K2 test demonstrated a photometric precision of 82 ppm for a 12th magnitude point source over 6-hr exoplanet transit timescales. This estimate was based on the K2 light curve in the right-hand panel. The dashed line represents the 1σ point-to-point (30-min) standard deviation of all data points. The red points are 6-hr averages of the data. The shaded regions represent data-collection periods where reaction wheel resaturations and fine-guidance tests made the data unusable. For comparison, a similar plot is provided on the left for a 12th magnitude G dwarf collected during the *Kepler* mission (note the scale change by ~4x).

TABLE 3

COMPARISON OF *KEPLER* AND K2 PHOTOMETRIC PERFORMANCE

Parameter[a]	*Kepler* (ppm)	K2 (ppm)
Standard Deviation (1σ)	99	404
6-hour phot. precision (ζ)	18	82

[a] Parameters determined as described in § 5. *Kepler* baseline photometric values are described in Koch et al. (2010).

precision. The *Kepler* sample consists of quiet G dwarfs, selected randomly across the field of view. The K2 sample is also selected randomly across the full field-of-view; however, the nature of each target is unknown. It is unlikely they are all quiet dwarfs, resulting in the scatter observed in the distribution.

As part of an early science demonstration with K2, WASP-28 was observed for 2.6 days in short cadence (1-minute sampling) mode during an engineering test in 2014 January. WASP-28 is a 12th magnitude, Sun-like star with a somewhat subsolar metallicity and known to host a Jupiter-sized exoplanet with an orbital period of 3.4 days (Anderson et al. 2014).

The K2 light curve (Fig. 11) was extracted from calibrated pixel data using an elliptical aperture that was allowed to recenter its position between exposures. In each exposure, we removed a local background determined from the median flux in nearby pixels. Finally, we passed the data through a median filter with a 1-day window.

Near the end of our short observation, we observed a single transit of the planet WASP-28b as it moved across the host star. We fit a limb-darkening transit model (Mandel & Agol 2002) to our observations and obtained planet parameters consistent with published values (Anderson et al. 2014). The residuals of the transit fit to the data show a point-to-point (rms) scatter of 0.16%. This equates to a 6-hr integrated noise level of 84 ppm.

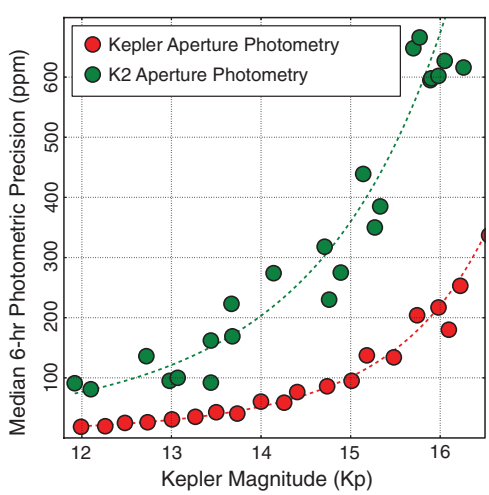

FIG. 10.—The 2013 December on-orbit K2 test demonstrated a photometric precision within a factor 3–4 times that of *Kepler*. The plot above provides the *Kepler* and K2 median 1σ sensitivities to 6-hr transits (ζ) as a function of target magnitude.

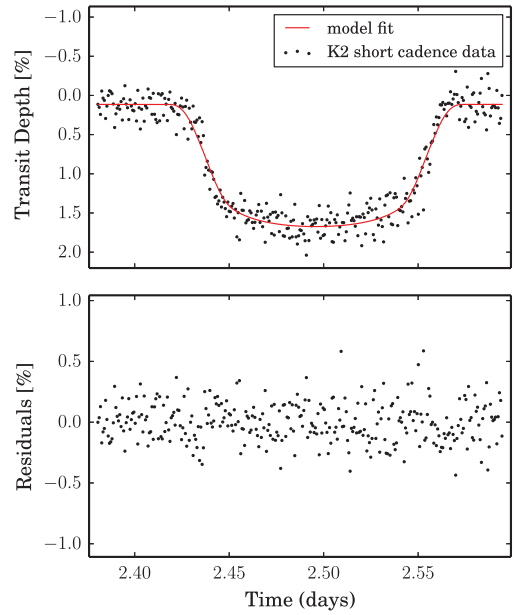

FIG. 11.—K2 light curve of the transiting exoplanet WASP-28b. During a 2.6-day science verification period, contained within our 2014 January engineering test, we obtained 1-minute sampled observations of the 12th magnitude target star. K2 observations are shown in black and the best fitting transit model in in red. The residuals (*bottom panel*) of the transit fit to the data show a point-to-point (rms) scatter, for a 6-hr integrated noise level, of 84 ppm.

6. CONCLUSION

K2 is a new mission both in spacecraft control and science opportunity. It makes use of the existing *Kepler* spacecraft and the large-area focal plane array to provide high-precision, long-duration photometric observations, allowing new scientific discoveries in many areas of astrophysics. K2 is currently undergoing Campaign 0 and, if approved by NASA, is planned to continue observing a new field approximately every 3 months starting around 2014 June 1. K2's photometric precision and observing ability will far exceed ground-based telescopes and enable discoveries of high-value transiting exoplanets, a variety of aspects in stellar evolution, and new windows to explore in extragalactic science. Observing four to five 75-day campaigns each year, K2 will scrutinize the sky along the ecliptic plane.

K2's key science objectives were laid out above (§ 3) and we have presented early science results (§ 5) attesting to the mission's ability to carry out these goals. K2 is a low-cost space astrophysics mission capable of elucidating many aspects in stellar astrophysics across the H-R diagram and providing detailed observations of variable galaxies and early time observations of supernovae. In addition, K2's unique exoplanet survey will fill the gaps in duration and sensitivity between the *Kepler* and TESS missions, and offers prelaunch exoplanet target identification for JWST transit spectroscopy.

We thank Andy Adamson, Michael Bicay, Padi Boyd, Alex Brown, Jessie Dotson, Nick Gautier, Doug Gies, Richard Green,

Steve Kawaler, Caty Pilachowski, and Dave Silva for reading early drafts and making comments that led to a better paper. C. Aerts, S. Basu, T. Bedding, K. Brogaard, J. Christensen-Dalsgaard, S. Kawaler, H. Kjeldsen, D. Kurtz, and D. Stello are acknowledged for making valuable contributions to the work involved in this paper. The authors also wish to thank Wendy Stenzel for producing the graphics associated with this paper and Mark Messersmith for keeping us in line during the work. Ball Aerospace is gratefully acknowledged for their long-term commitment to *Kepler* and now K2.

REFERENCES

Anderson, D. R., Collier Cameron, A., Hellier, C., et al. 2014, A&A, in press (arXiv:1402.1482)
Aerts, C., Thoul, A., Daszynska, J., et al. 2003, Science, 300, 1926
Aerts, C., Zwintz, K., Marcos-Arenal, P., et al. 2013, Kepler white paper
Albrecht, S., Winn, J. M., Johnson, J. A., et al. 2012, ApJ, 757, 18
Arevalo, P., Uttley, P., Lira, P., et al. 2009, MNRAS, 397, 2004
Beichman, C., Ciardi, D., Akeson, R., et al. 2013, in press (arXiv:1309.0918)
Bell, C. P. M., et al. 2012, MNRAS, 424, 3178
Borucki, W. J., et al. 2010, Science, 327, 977
Boudreault, S., et al. 2012, MNRAS, 421, 3419
Breedt, E., McHardy, I. M., Arevalo, P., et al. 2010, MNRAS, 403, 605
Brucalassi, A., Pasquini, L., Saglia, R., et al. 2014, A&A, 561, L 9
Chaplin, W. J., & Miglio, A. 2013, ARA&A, 51, 353
Charbonneau, D., Berta, Z. K., Irwin, J., et al. 2009, Nature, 462, 891
Ciardi, D. R., Fabrycky, D. C., Ford, E. B., et al. 2013, ApJ, 763, 41
Crockett, C. J., Mahmud, N. I., Prato, L., et al. 2012, ApJ, 761, 164
Degroote, P., Aerts, C., Baglin, A., et al. 2010, Nature, 464, 259
Dias, W. S., et al. 2012, A&A, 539, 125
Dong, S., Gould, A., Udalski, A., et al. 2009, ApJ, 695, 970
Dressing, C. D., & Charbonneau, D. 2013, ApJ, 767, 95
Edelson, R., & Malkan, M. 2012, ApJ, 751, 52
Edelson, R., Mushotzky, R., Vaughan, S., et al. 2013, ApJ, 766, 16
Fressin, F., Torres, G., Charbonneau, D., et al. 2013, ApJ, 766, 81
Gaidos, E., Fischer, D. A., Mann, A. W., & Howard, A. W. 2013, ApJ, 771, 18
Gallet, F., & Bouvier, J. 2013, A&A, 556, A 36
Gillen, E., Aigrain, S., McQuillan, A., et al. 2014, A&A, in press (ArXiv 1311.3990)
Gould, A. 1999, ApJ, 514, 869
Gould, A., & Horne, K. 2013, ApJ, 779, L 28
Gould, A., & Loeb, A. 1992, ApJ, 396, 104
Gressel, O., Nelson, R. P., Turner, N. J., & Ziegler, U. 2013, ApJ, 779, 59
Hayden, B. T., Garnavich, P. M., Kasen, D., et al. 2010, ApJ, 722, 1691
Howard, A., Marcy, G., Bryson, S., et al. 2012, ApJS, 201, 15
Irwin, J., & Bouvier, J. 2009, in IAU Symp. 258, The Ages of Stars, ed. E. E. Mamajek, D. R. Soderblom, & R. F. G. Wyse (New York: Cambridge), 363
Janes, K., et al. 2013, ApJ, 145, 7
Kasen, D. 2010, ApJ, 708, 1025
Klahr, H. 2008, NewAR, 52, 78
Klahr, H., & Kley, W. 2006, A&A, 445, 747
Koch, D., Borucki, W., Basri, G., et al. 2010, ApJ, 713, L 79
Kopparapu, R. K. 2013, ApJ, 767, L 8
Lissauer, J. J., Hubickyj, O., D'Angelo, G., & Bodenheimer, P. 2009, Icarus, 199, 338
McNamara, B., et al. 2012, AJ, 142, 53
Mandel, K., & Agol, E. 2002, ApJ, 580, 171
Marcy, G. W., Isaacson, H., Howard, A. W., et al. 2014, ApJS, 210, 20
Marley, M. S., Fortney, J. J., Hubickyj, O., et al. 2007, ApJ, 655, 541
Meibom, S., Torres, G., Fressin, F., et al. 2013, Nature, 499, 55
Michaud, G., Richer, J., & Richard, O. 2013, Astron. Nachr., 334, 114
Miglio, A., Chiappini, C., Morel, T., et al. 2013, MNRAS, 429, 423
Mushotzky, R. F., Edelson, R., Baumgartner, W., & Gandhi, P. 2011, ApJ, 743, L 12
Nakar, E., & Sari, R. 2010, ApJ, 725, 904
Olling, R., Tucker, B., Shaya, E., et al. 2013, Kepler white paper
Pecaut, M. J., et al. 2012, ApJ, 746, 154
Petigura, E. A., Howard, A. W., & Marcy, G. W. 2013, Proc. Natl. Acad. Sci., 110, 19273
Piskunon, A. E. 2011, A&A, 525, 122
Putnam, D., & Wiemer, D. 2014, Journal of the Astronautical Sciences, AAS, 14–102
Quinn, S. N., White, R. J., & Latham, D. W., et al. 2012, ApJ, 756, L 33
Raymond, S. N., Mandell, A. M., & Sigurdsson, S. 2006, Science, 313, 1413
Rebull, L., et al. 2012, ApJS, 186, 259
Ridgway, S., et al. 2014, ApJ, in press
Santos-Silva, T., & Gregorio-Hetem, J. 2012, A&A, 547, 107
Savitzky, A., & Golay, M. J. E. 1964, Anal. Chem., 36, 1627
Schilbach, E., & Roser, S. 2012, A&A, 537, 129
Spiegel, D. S., & Burrows, A. 2012, ApJ, 745, 174
Stello, D., Huber, D., Bedding, T. R., et al. 2013, ApJ, 765, L 41
Van Eyken, J. C., Ciardi, D.i R., von Braun, K., et al. 2012, ApJ, 755, 42
Woosley, S. E., Kasen, D., Blinnikov, S., & Sorokina, E. 2007, ApJ, 662, 487